



**Journal of Engineering  
Sciences Assiut University  
Faculty of Engineering**

**Vol. 49, No. 1**

**January 2021**

**PP. 085 – 106**



**NUMERICAL STUDY OF FLANGE BUCKLING  
BEHAVIOR OF HIGH-STRENGTH STEEL  
CORRUGATED WEB I-GIRDERS**

**Amr B. Saddek<sup>1,2</sup>, Sedky A. Tohamy<sup>3</sup>, Amr Elsayed<sup>4</sup>, Ahmed A.M. Drar<sup>5</sup>**

<sup>1</sup> *Assoc. Prof., Civil Engineering Department, Albaha University, Saudi Arabia.  
E-mail: amro@bu.edu.sa*

<sup>2</sup> *Assoc. Prof., Civil Engineering Department, Beni-suef University, Egypt.  
E-mail: amr01174@eng.bsu.eg*

<sup>3</sup> *Professor, Civil Engineering Department, Minia University, Egypt.  
E-mail: Sedky\_t2000@yahoo.com*

<sup>4</sup> *Demonstrator, Civil Department, Faculty of Engineering, Sohag University, Egypt.  
E-mail: amrelsayed895@gmail.com (Corresponding Author)*

<sup>5</sup> *Assist. Prof., Civil Department, Faculty of Engineering, Sohag University, Egypt.  
E-mail: attva85@yahoo.com*

*Received 28 December 2020; Revised 05 February 2021; Accepted 06 February 2021*

**Abstract**

Steel plate girders with trapezoidal corrugated webs (TCWPGs) have been used over the last years around the world in many roadway and railway steel bridges as they can introduce several important advantages compared to flat web plate girders. The proper design of corrugated web girders depends mainly on the flexural and shear capacity of them. However, the flexural capacity is more important. Also, not many researchers studied the flexural capacity of such girders especially, when flange local buckling failure type (FLB) occurs in these corrugated web girders. In this paper, the flange local buckling behavior of steel trapezoidal corrugated web girders built up from high-strength steel (HSS) plates has been investigated to get the advantages of both

the technique of corrugated web plates (CWPs) and the high-strength steel material (HSSs) together. A new numerical parametric study on four important parameters has been carried out to explain and investigate the flange local buckling behavior of high-strength steel corrugated web girders, considering mainly the influences of the flange to web thickness ratio, unsupported length of the compression flange, the corrugation angle and the initial imperfection magnitude of the compression flange on the behavior of girders with corrugated webs built up from HSSs. Using the commonly used finite element software ABAQUS, the results of the FE models have been obtained to be analyzed and discussed. Finally, some important advices have been introduced to aid the structural engineers to design such girders under flexural loading in economical manner.

**KEYWORDS:** Flexural behavior; flange local buckling (FLB); trapezoidal corrugated web (TCW); high-strength steel (HSSs); ABAQUS/CAE.

---

## 1. Introduction

Corrugated web steel plate girders have been commonly used in bridges construction for long years. Design of these girders is controlled by two main design capacities; first is the shear design capacity which depends on the corrugated web, second is the flexural design capacity which depends on the upper and lower flanges. Due to the accordion effect, the corrugated webs only resist the shear forces and the flanges resist the bending moment [1]. The use of HSSs in the corrugated web girders provides several structural benefits such as the use of thinner steel plates resulting in reduced structural weight, lower construction cost and easier transportation processes. A lot of steel bridges were built up by using HSSs in the most of countries around the world. The concept of HSSs is that steels with a nominal yield strength  $f_y \geq 460$  MPa [2]. The properties of high-strength steel stress-strain are completely different from the properties of commonly used and investigated normal strength steels (NSSs). High-strength steels have a gradual elastic portion unlike normal strength steels which have a sharp yield point and yield plateau. The part of strain hardening in HSSs is reduced than NSSs and a high yield ratio (YR) exceeds 0.9 is found in the characteristics of HSSs. Therefore, in numerical studies, the behavior of material of HSSs is always modelled

by elastic-perfect plastic bilinear curves [3], [4]. Figure (1) shows examples for constructed bridges built up from HSSs.



(a) The Millau Viaduct in France



(b) The Ilverich Bridge in Germany



(c) Bridge in Zuid Beveland



(d) The Prince Clause Bridge, Utrecht

Figure (1) – Examples of S460 - HSSs constructed bridges [5]

In the literature, trapezoidal corrugated web girders have been investigated and analyzed under bending moment. It has been noticed that the failure may be the lateral-torsional buckling or the local flange buckling. If the girders were laterally restrained so the lateral-torsional buckling type failure cannot occur, and they fail only by local flange buckling failure type. In the last twenty years, the flange buckling strength of trapezoidally corrugated web girders has been studied numerically and experimentally. In 1956, NACA [6] started the research on the connected riveted angle built-up sections of the corrugated web steel girders in wings of airplanes. A lot of researchers studied the structural behavior of corrugated web girders; however, very little research was carried out on the flange buckling behavior and the ultimate bending moment strength of steel girders with thin flanges.

Results of previous research proved that the accompanying shear force has no effect on the bending moment strength [1], [7]–[9] and only

the flanges contribute in the bending moment capacity [1], [10], [11]. In 1997, Elgaaly et al. [1] tested six specimens of corrugated web beams to failure under uniform bending moment. The specimens failed by the vertical inelastic buckling of the compression flange. The results of the test proved that the corrugated webs have no ability to resist any bending moments. A finite element modeling of test specimens has been carried out using the FE program ABAQUS using the nonlinear analysis. Parametric studies were performed to investigate the corrugation configuration, the effect of the ratio between the flange and web thicknesses and yield stresses and the panel aspect ratio. Their studies concluded that for design purposes, the ultimate moment capacity of the corrugated web beams can be calculated based on the flange yielding and the corrugated web offered a negligible contribution due to the accordion effect. In 1997, Johnson and Cafolla [12] tested five specimens of corrugated web beams. The local flange buckling was the failure mode of three of the specimens and the web shear buckling was the mode of failure of the other specimens. According to the results of the test, the authors propose that to calculate the flange plate slenderness, the average flange outstand ( $b_f/2$ ) should be used if Eq. (1) satisfies.

$$R = \frac{(b+d) d \cdot \tan \alpha}{(b+2d) b_f} < 0.14 \quad (1)$$

Where R is the enclosing effect of the trapezoidal web, b is the width of the horizontal web panel, d is the horizontal projection of the inclined panel width of the trapezoidal web,  $\alpha$  is the corrugation angle,  $b_f$  is the width of the flange.

In 2006, Dabon and Elamary [13] executed experimental investigation on two specimens with corrugated webs subjected to bending. A comparison between corrugated web beams and flat web beams was performed to show the advantages and disadvantages of using web corrugation. In 2007, Sayed-Ahmed [14] investigated the local flange buckling of corrugated web girders using a parametric linear buckling analysis. The analysis results concluded that the coefficient of buckling limited to  $k = 0.7$  and the compression flange classification should depend on the larger outstand distance of the corrugated web girder's flange. In 2014, Lho et al. [15] tested four trapezoidal corrugated specimens with slender webs. They investigated the maximum ratio of web slenderness to avoid the flange induced buckling to occur in the

compression flange. Also, a linear analysis of buckling has been performed on these specimens. The experimental results concluded that the maximum ratio of web slenderness could be 1.5 times larger than the ratio proposed by DAST-Richtlinie 015 [11].

In 2015, Li et al. [16] executed experimental and numerical investigations on six corrugated web specimens with wide flange subjected to normal stresses. Their work aimed to specify the limiting ratio of outstand distance of the compression flange to thickness and the evaluation of the coefficient of buckling depending on the average outstand distance of the flange. Firstly, they calibrated the coefficient of buckling and the ratio of outstand distance to thickness using the linear buckling analysis, then they modified the flange's classification limit based on the results of the nonlinear finite element analysis by considering the effect of both geometric imperfections and residual stresses. In 2017, Jáger et al. [17], [18] carried out experimental and numerical studies on trapezoidal corrugated web girders subjected to pure bending moment to investigate the flange buckling behavior of these girders type. They also proposed a new equation to calculate the local buckling coefficient of the flange considering some omitted effects which should be considered.

The previous research studies show that some of important parameters have not been studied in the investigation of the local flange buckling behavior of trapezoidal corrugated web girders built up from HSSs subjected to pure bending moment. In the current study, some important parameters which control the flange buckling behavior of HSSs-TCWPGs have been investigated numerically. Also, some important advices have been introduced to help the design engineers to choose the geometrical properties carefully to obtain an economical design of these type of girders.

## **2. Validation of the current FE numerical model**

### **2.1 General**

The FE program ABAQUS [19] was used to simulate trapezoidal corrugated web plate girders built up from HSSs using geometries and material properties. For members sensitive to buckling, two subsequent analyses are required in the FE analysis. The first analysis is the

eigenvalue buckling analysis is used to obtain the buckling modes of these members, then a load-displacement nonlinear analysis has been performed to include the initial geometrical imperfections and material nonlinearity. The nonlinear analysis has been used to predict the failure modes, ultimate loads and load-deflection relationships. In the eigenvalue analysis, the first positive buckling mode has been used as the shape of the initial imperfection [20]. Experimental test of Jáger et al. [17] has been used to develop a FE model to be used in the current numerical parametric study. To validate the FE model, both the results of the experimental test and the numerical analysis results have been compared to specify the accuracy of the developed model. The experimental test was a four-point bending loading test on 16 large scale simply supported specimens. The geometric properties are shown in Figure (2).

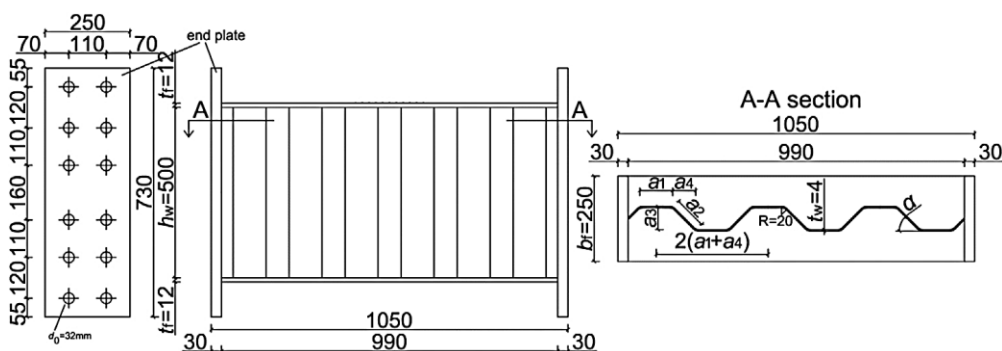


Figure (2) Geometric properties of trapezoidal corrugated web girder [17]

## 2.2 Loading method and boundary conditions

In the current finite element model, the used boundary conditions were hinged support on one side of the girder where the displacements were restrained in x-, y-, z-directions, roller support on the other side where the displacements were restrained in y-, z-directions. The girders are loaded statically by two concentrated loads. Vertical stiffeners at supports and concentrated loads location have been used. The girders were restrained laterally at the concentrated loads location to prevent the girders from failing by lateral-torsional buckling. Figure (3) shows the boundary conditions and load application points of the FE model used in the current study.

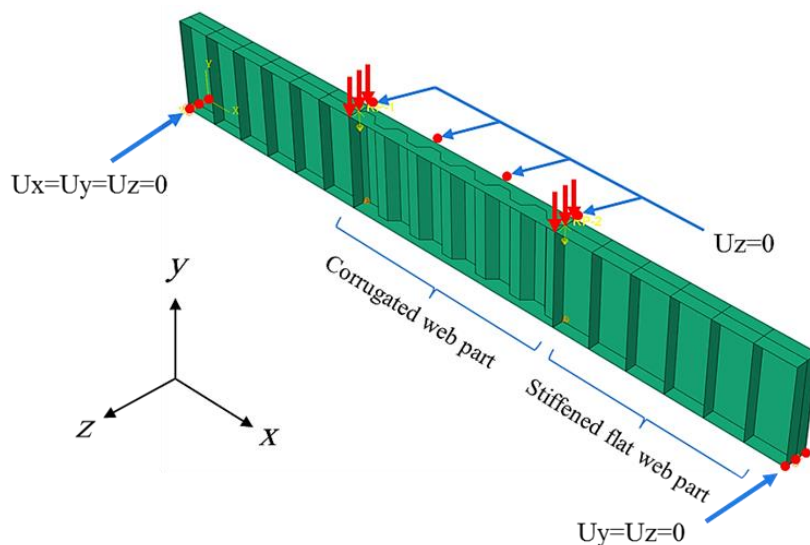


Figure (3) – Boundary conditions, load application points and lateral restraints of FE model

## 2.3 Convergence study

Convergence study is performed to study the suitable mesh size and type of meshing to be considered in the FE model to get accurate and converged results. In the experimental test of Jáger et al. [17], two test specimens have been used in the convergence study to study the suitable type and size of the used mesh in the numerical parametric study.

### 2.3.1 Element type, meshing and initial imperfection magnitude

In the current study, a 4-node doubly curved thin or thick shell, reduced integration, hourglass control, finite membrane strains (S4R) element has been used to simulate the steel plates failing by buckling. The element has four nodes each of them has six degrees of freedom; three are translational degree of freedom ( $U_1$ ,  $U_2$ ,  $U_3$ ) and three are rotational degree of freedom ( $UR_1$ ,  $UR_2$ ,  $UR_3$ ). Figure (4) indicates the S4R element used in the FE mesh of a typical corrugated web plate girder. Two types of meshing have been used in the convergence study; the first type is the mapped mesh in which a regular, structured, and uniform meshing has been considered and the second type is the free meshing in which a random and irregular meshing has been considered as shown in Figure (5).

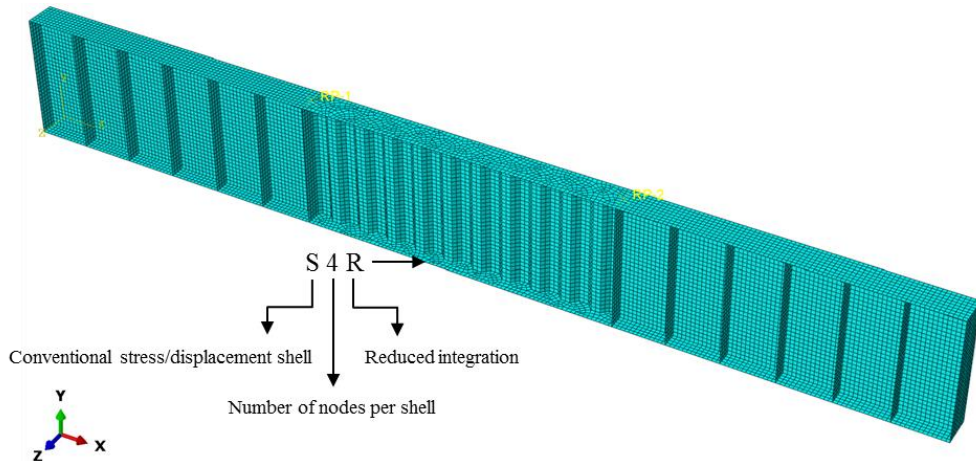


Figure (4) – FE mesh of a typical CWPGs

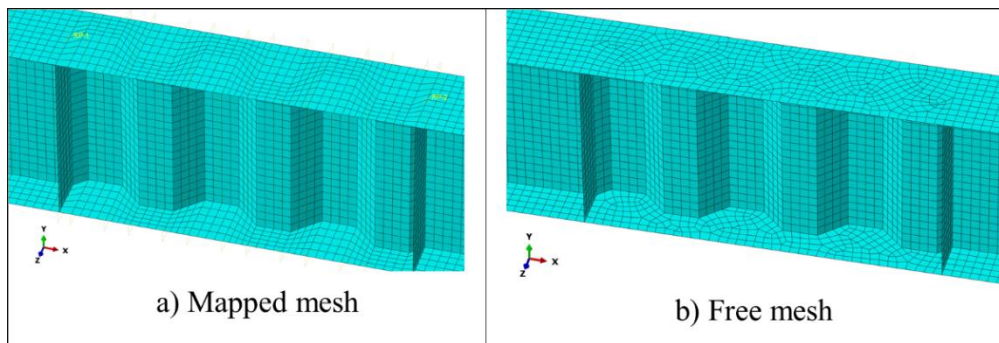


Figure (5) – Mapped and free meshing types

Figure (6) presents the differences between mapped and free meshing types and the effect of each of them on the accuracy of results of the FE modeling at various mesh sizes compared to test results. It is obvious from the comparisons that the free mesh is more accurate than the mapped one at all sizes of meshing except for size of 30mm in the slender flange model ( $C_f/t_f = 20$ ) in Figure (6-a), however this model does not represent the numerical models investigated in the current parametric study as these models have lower flange slenderness ratios ( $C_f/t_f \leq 17$ ). So free meshing type has been used in the FE modeling to save the analysis time.

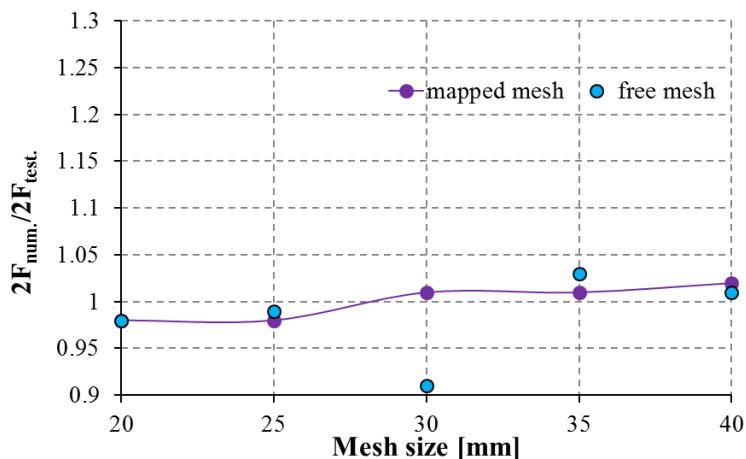
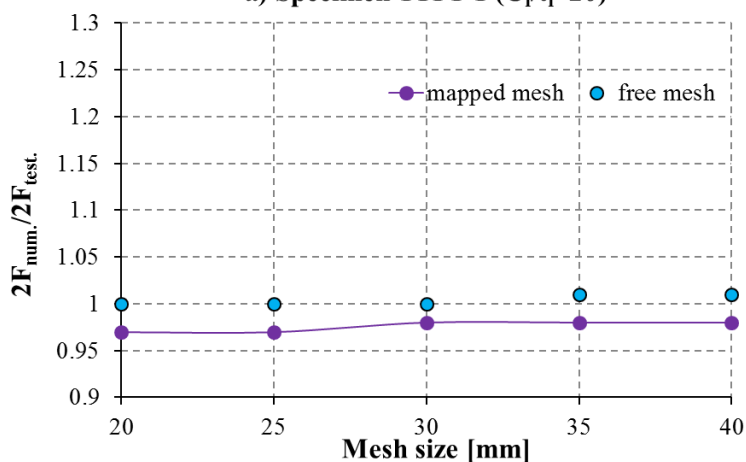
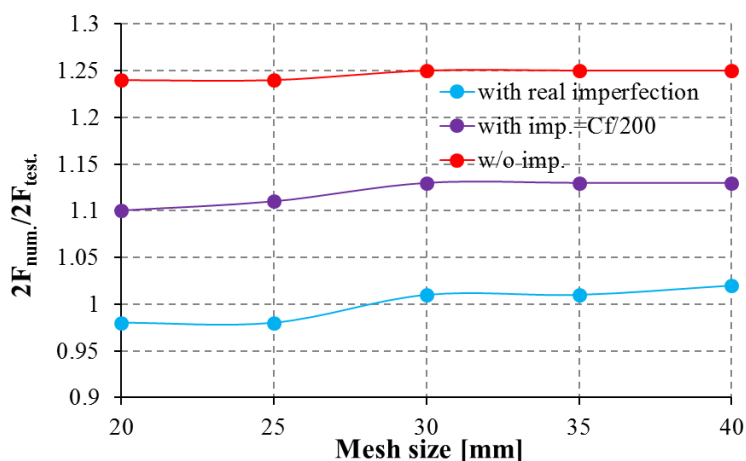
a) Specimen 1TP1-1 ( $C_f/t_f \approx 20$ )b) Specimen 8TP2 ( $C_f/t_f \approx 14$ )

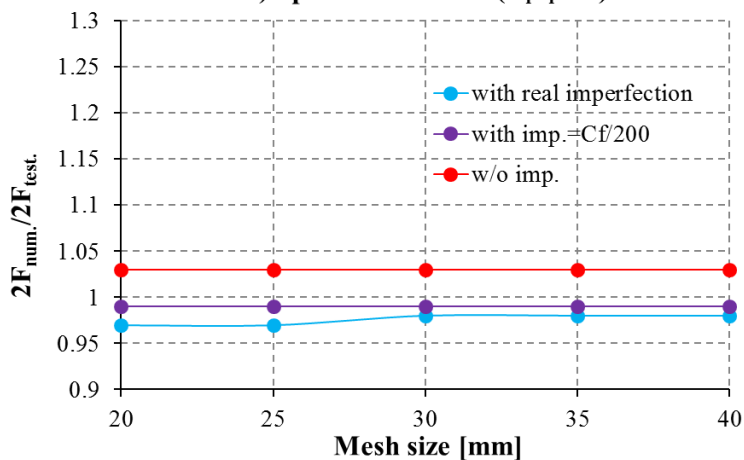
Figure (6) – Convergence study of meshing type sensitivity

Figure (7) presents the results of convergence study that has been made on two test specimens in the experimental test, one of them with slender flange and the other with stocky flange (1TP1-1 and 8TP2, respectively). Relationship between the numerical to experimental total applied load ratio on the vertical axes and the mesh size on the horizontal axes is plotted at various values of initial imperfection magnitudes. In the specimen with slender compression flange ( $C_f/t_f \approx 20$ ) higher accuracy of results from the numerical model has been obtained using the real initial imperfections measured from test, and the size of mesh between 25 to 30 mm gives the best results. Also, larger imperfection sensitivity is obtained in the slender flange specimen. On the other side in specimen

with stocky flange ( $C_f/t_f \approx 14$ ) the mesh size has almost no effect on the accuracy of the results. Also, this specimen is less sensitive to the initial imperfection magnitude and higher accuracy of results has been obtained by using  $C_f/200$  as initial imperfection magnitude. Based on the convergence study of initial imperfection magnitude the value of the initial imperfection recommended by EC3 [21] for flanges subjected to twist ( $C_f/50$ ) gives lower accurate results compared to the test results in case of girders failed by flange local buckling. Based on the results of the convergence study, a mesh size of 25mm has been used in the numerical analysis of the current study to get accurate results and saving analysis time also.



a) Specimen 1TP1-1 ( $C_f/t_f \approx 20$ )



b) Specimen 8TP2 ( $C_f/t_f \approx 14$ )

Figure (7) – Convergence study of mesh size and initial imperfection magnitude sensitivity

## 2.4 Material constitutive model

In this FE analysis, the high strength steel S460 has been used. S460 has 460 MPa yield strength and 540 MPa ultimate strength. In the numerical analysis, the material behavior of HSSs is usually idealized by elastic-perfect plastic bilinear curves [3], [4] as previously discussed in the introduction. Elkawas et al. [22] examined this assumption considering three different constitutive models. The first material model is the elastic-perfect plastic, the second is the elastic-plastic with strain hardening material model and finally the tri-linear stress-strain curves. The same girders' responses have been obtained from the three curves. So, based on the results of this comparison, the elastic-perfect plastic stress-strain curve has been used in the current FE analysis to simulate the real behavior of HSSs as shown in Figure (8). The elastic modulus ( $E$ ) has been assumed equal to 210,000 MPa and taking the Poisson's ratio of steel ( $\nu$ ) as 0.3. The relationship of the high-strength steel material has been modelled as a Von Mises material with an isotropic hardening.

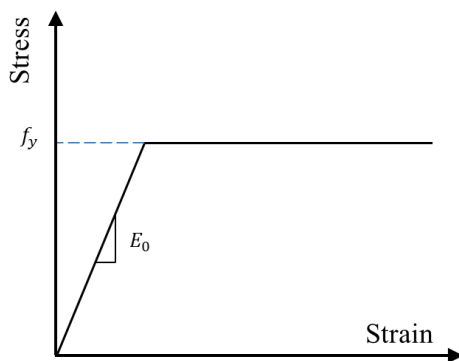


Figure (8) – Elastic-perfect-plastic stress-strain curve for HSSs

## 2.5 Modelling of Equivalent Geometrical Imperfections

To simulate the initial imperfections and residual stresses which caused by the cutting and welding processes operated on the built-up sections, the equivalent geometrical imperfections should be added to the perfect FE model. The first step of the FE analysis is the linear buckling analysis which is used to generate the expected buckling failure modes (eigenmodes) as shown in Figure (9). In the next step, the nonlinear FE analysis has been carried out to get the ultimate resistance of the girders. The first positive buckling mode has been used as the shape of the imperfection [23]. In the current FE analyses, the coordinates of the

eigenmode obtained from the linear buckling analysis have been scaled with the maximum allowed value of equivalent geometrical imperfection ( $C_f/50$ ) suggested by the EC3 [21].

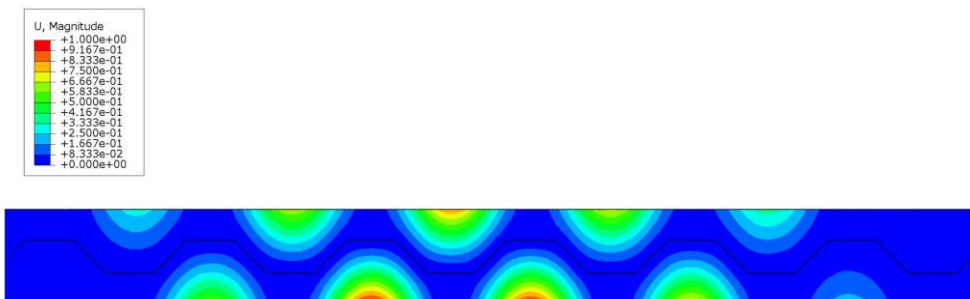


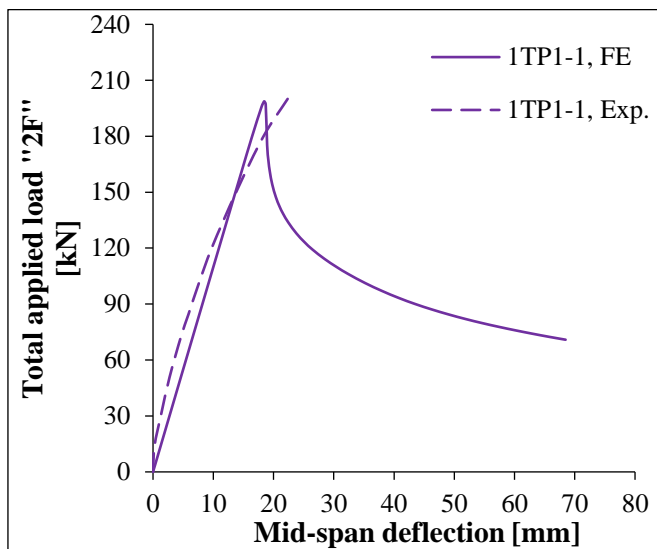
Figure (9) – First positive buckling mode used as imperfection shape

## 2.6 Validity of the current FE model

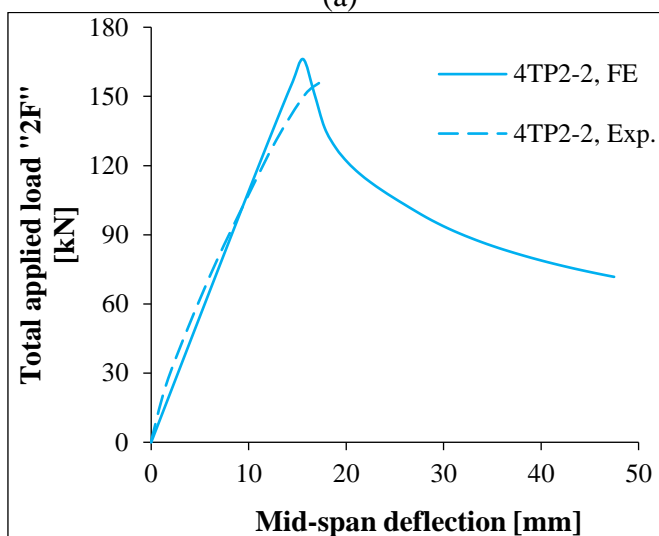
The accuracy of the current FE model has been checked by analyzing six test specimens [17]. Total applied load (2F) and mid-span deflection have been plotted on curve based on the numerical and experimental results as shown in Figure (10). The comparisons between the numerical and experimental loads are listed in Table (1). Small differences between the numerical and experimental loads have been noticed in all current validated specimens except 5TP2-1 specimen as the measured maximum imperfection magnitude of this specimen is not declared clearly by the author [17], this comparison reflects that the current FE model represents the real behavior of CWPGs built up from HSSs.

Table: 1. Comparison between numerical and experimental load carrying capacities

No.	Specimen	2F (Exp.) kN	2F (Num.) kN	Difference %
1	1TP1-1	200.5	198.7	0.9
2	4TP2-1	148.7	159.3	7.1
3	4TP2-2	156.3	166.2	6.3
4	5TP2-1	172.1	194	12.8
5	8TP2	306.2	297.4	2.9
6	9TP3	326.3	314.9	3.5



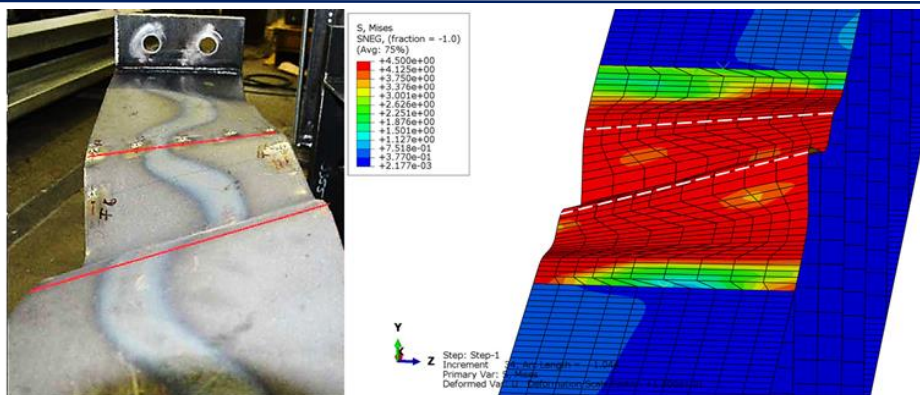
(a)



(b)

Figure (10) – Total applied load versus mid-span deflection curves for specimens: (a) 1TP1-1, (b) 4TP2-2

Figure (11) shows a comparison between the failure mode of the specimen in the experimental test and in the numerical analysis. It is obvious from the comparison between the experimental and numerical failure mode that the FE model can expect accurately the flange local buckling failure mode of the corrugated web steel girders built up from HSSs.



(a) Experimental failure mode

(b) Numerical failure mode

Figure (11) – Experimental versus numerical failure mode of Specimen 1TP1-1

### 3. Numerical Parametric Study

In this paper, a numerical parametric study has been carried out based on the validated numerical model to investigate the flange local buckling behavior of trapezoidal corrugated web steel plate girders built up from high-strength steel. Four parameters have been investigated using more than one hundred FE models to study the local flange buckling behavior of these girders. The investigated parameters are flange-to-web thickness ratio ( $t_f/t_w$ ), unsupported length of the compression flange ( $L$ ), corrugation angle ( $\alpha$ ) and initial imperfection magnitude ( $U$ ).

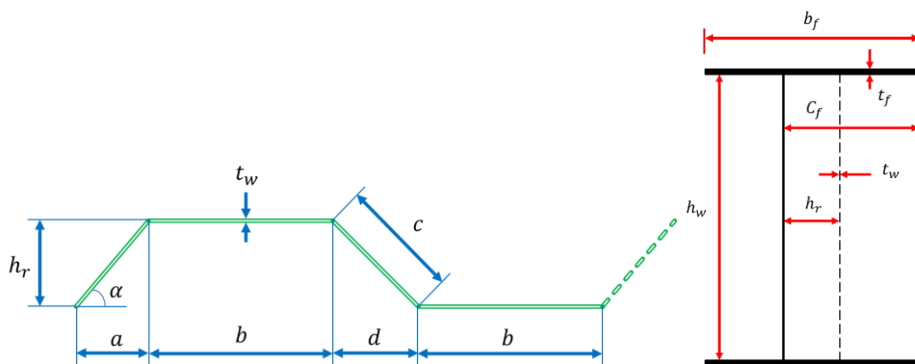


Figure (12) – Trapezoidal corrugated web profile and geometric notations of cross section

Figure (12) indicates the geometric notations of corrugated web profile and cross section of trapezoidal corrugated web girders; where  $C_f$  is the maximum outstand distance of the flange,  $h_r$  is the depth of corrugation and  $b_f$  is the width of the flange. In Figure (13), the layout of the investigated girders has been shown. The corrugated web part has been located between two stiffened flat web parts and two concentrated applied loads were located at the connection between flat and corrugated web parts in order to apply pure bending moment loading on the corrugated web part. Two analyses have been applied; first is the linear buckling analysis (LBA) to determine the critical compressive stress therefore the local buckling coefficient. Second is the geometrical and material nonlinear imperfect analysis (GMNIA) to investigate the ultimate bending moment capacity of corrugated web girders.

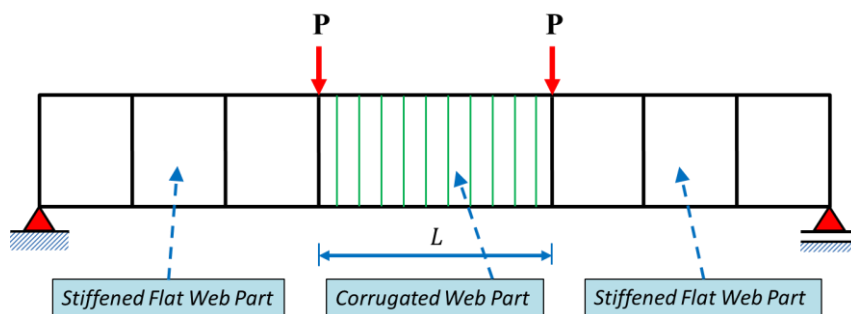


Figure (13) – Layout of current investigated corrugated web girder

The following range of investigated parameters has been considered:

- Flange-to-web thickness ratio ( $t_f/t_w$ ): 1:8
- Unsupported length of the compression flange ( $L$ ): 1000:7000 mm
- Corrugation angle ( $\alpha$ ): 30 – 37 – 45
- Initial imperfection magnitude ( $U$ ):  $0.1t_f - 0.5t_f - t_f - C_f/50 - C_f/200$

#### 4. Results and Discussions

Previous studies carried on the flange buckling behavior of CWPGs have some shortenings as previously mentioned in the introduction. The current study aims to overcome these shortenings through investigating the most important parameters affecting on the flange buckling behavior of trapezoidal corrugated web bridge girders built up from HSSs. The

following discussions have been done to explain the effect of the parameters on the local buckling coefficient of the compression flange and the bending moment strength of CWPGs built up from HSSs to get economical design for these girders under flexural loading.

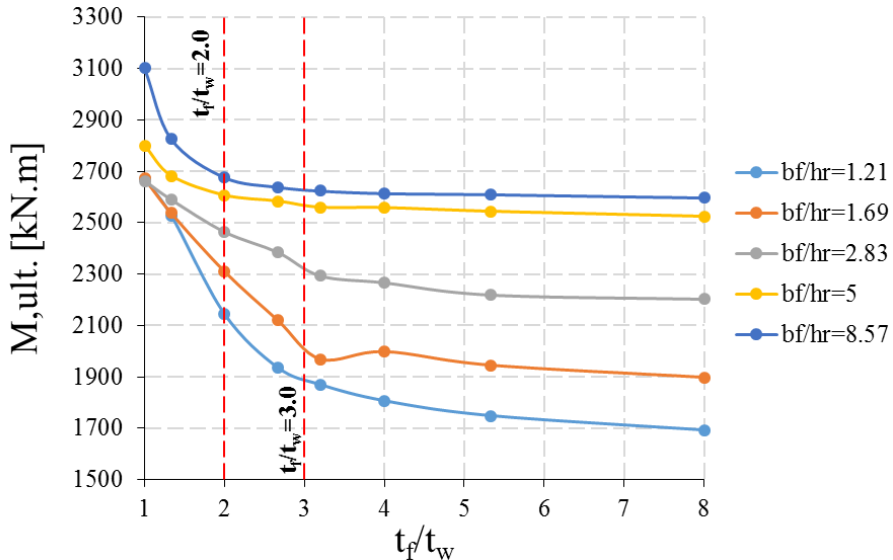


Figure (14) – Ultimate bending moment resistance versus flange-to-web thickness ratio

#### 4.1 Effect of flange-to-web thickness ratio ( $t_f/t_w$ )

The effect of flange to web thickness ratio has been shown in Figure (14). At  $b_f/h_r$  ratios  $\geq 5$ , the increase of  $t_f/t_w$  ratio decreases the ultimate bending moment capacity until  $t_f/t_w$  ratio equal to 2. On the other side, at  $b_f/h_r$  ratios  $< 5$ , the increase of  $t_f/t_w$  ratio decreases the ultimate bending moment capacity until  $t_f/t_w$  ratio equal to 3. As a result of this effect, the flange to web thickness ratio should not exceeds 3 in order to obtain higher bending moment resistances which are affected by the corrugated web thickness. Increasing the flange to web thickness ratio decreases the local flange buckling coefficient significantly up to  $t_f/t_w$  ratio equal to 3, then any increase in  $t_f/t_w$  ratio has no effect on the buckling coefficient as shown in Figure (15).

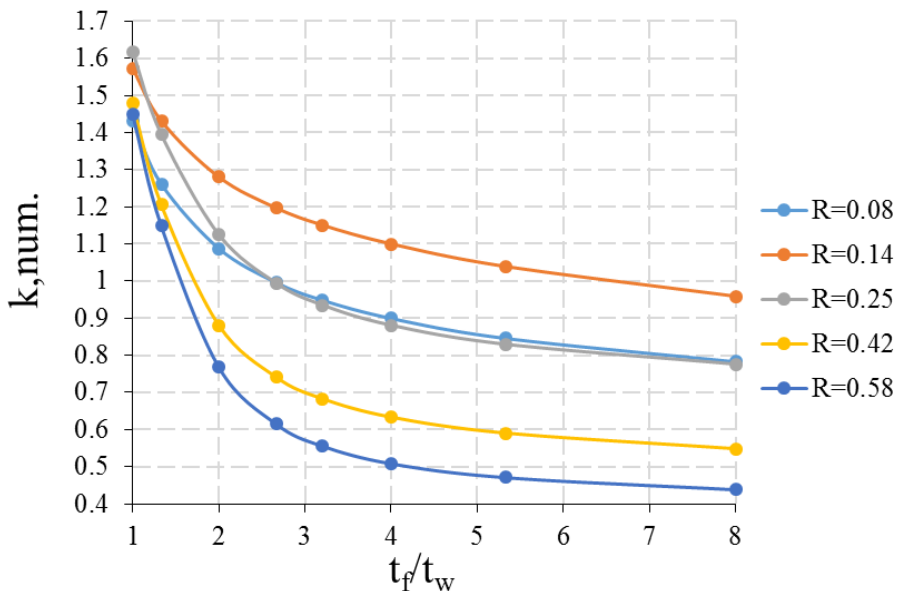


Figure (15) – Local buckling coefficient versus flange-to-web thickness ratio

#### 4.2 Effect of unsupported length of the compression flange (L)

The results of linear and nonlinear buckling analysis confirmed that the unsupported length of the compression flange has no effect on both the local buckling coefficient of the flange (See Figure (16)) and the ultimate bending moment strength (See Figure (17)) as the unsupported length of the compression flange has no effect on the local buckling failure of the subpanel of the compression flange as it is three sided supported by the corrugated web only.

#### 4.3 Effect of corrugation angle ( $\alpha$ )

Three values for angle of corrugation have been studied in the current numerical study. As shown in Figure (18), the corrugation angle of the corrugated web plate has a large effect on the bending moment resistance of trapezoidal corrugated web girders at ratios of  $b_f/h_r < 5$ , however the corrugation angle  $\alpha = 37$  is the best angle to get bending moment resistances higher than corrugation angles  $\alpha = 30$  and  $\alpha = 45$ . It is worth noting that the angle of corrugation  $\alpha = 37$  enabled the corrugated web to behave as a more rigid support to prevent the flange from failing by FLB failure type. On the other side, the corrugation angle has almost no effect on the bending moment resistance at  $b_f/h_r \geq 5$ .

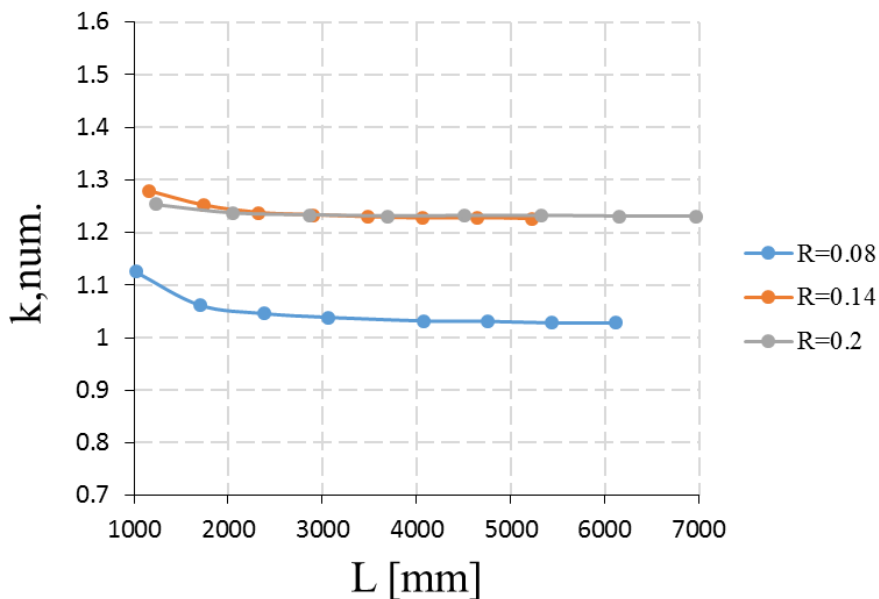


Figure (16) – Local buckling coefficient versus compression flange unsupported length

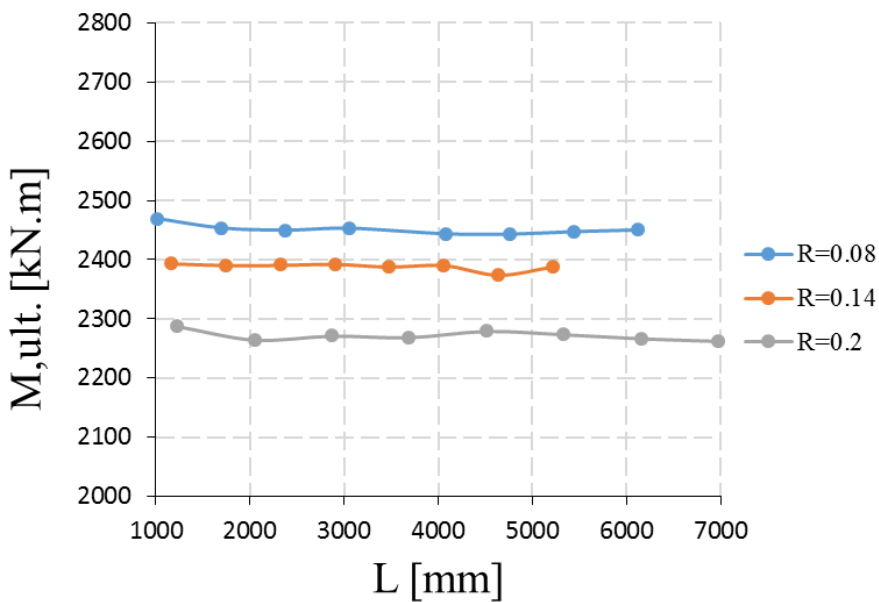


Figure (17) – Ultimate bending moment resistance versus compression flange unsupported length

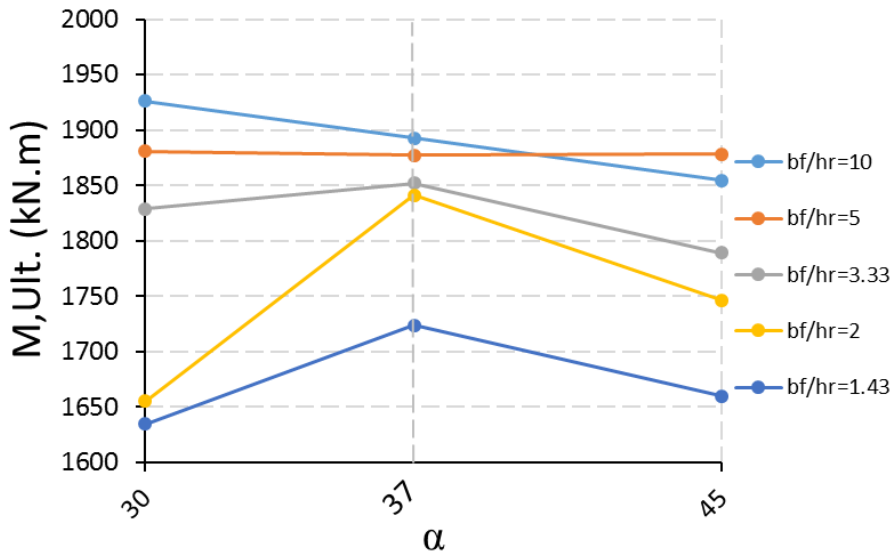


Figure (18) – Ultimate bending moment resistance versus corrugation angle

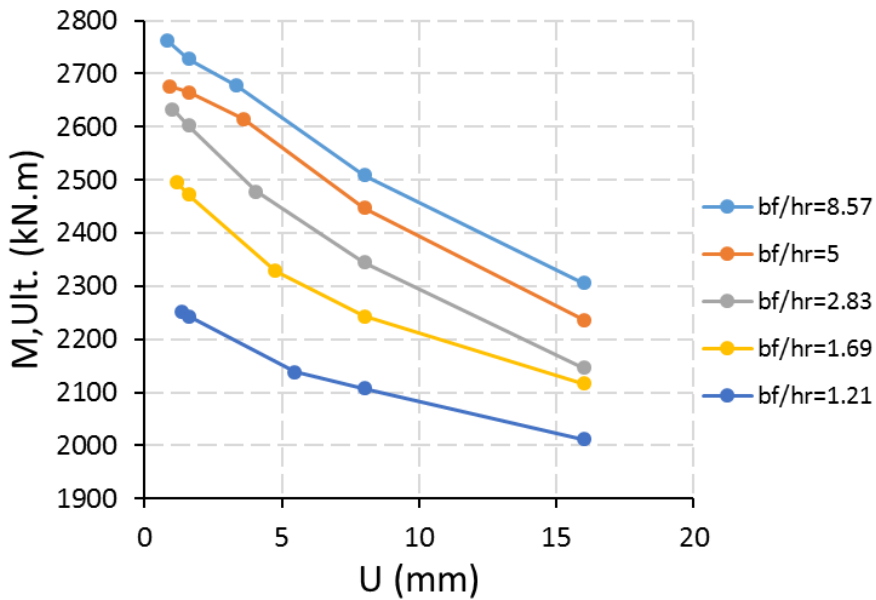


Figure (19) – Ultimate bending moment resistance versus initial imperfection magnitude

#### 4.4 Effect of initial imperfection magnitude (U)

The manufacturing and welding processes of steel corrugated web plate girders caused some imperfections in the plates of the cross section causing a decrease in the bending moment resistance. The effect of initial

imperfection magnitude on the ultimate bending moment resistance has been shown in Figure (19). Increasing the initial imperfection magnitude results in decreasing the moment capacity of the trapezoidal corrugated web girders significantly. Also, the slenderness of the flange has a large effect on the bending moment resistance at different magnitudes of initial imperfection as increasing the flange slenderness decreases the bending moment resistance at the same value of initial imperfection.

## 5. Summary and Conclusions

Based on the results of the current numerical parametric study carried out on trapezoidal corrugated web steel plate girders built up from HSSs to investigate the flange buckling resistance and the buckling behavior of these girders, the following concluded remarks may be summarized:

1. The effect of flange to web thickness ratio on both the flange buckling coefficient and the bending moment resistance was found to be significant up to flange to web thickness ratio ranges from 2 to 3.
2. The compression flange unsupported length has no effect on both the flange buckling coefficient and the ultimate bending moment resistance of trapezoidal corrugated web steel girders as the failure load was affected by the flange sub-panel properties and was not affected by the unsupported length of compression flange.
3. The corrugation angle  $\alpha = 37$  gives higher values of bending moment resistance than any other corrugation angle.
4. The corrugated web plate girders built up with high-strength steels are very sensitive to initial geometric imperfections.
5. The increase in flange slenderness significantly decreases the ultimate bending moment resistance of trapezoidal corrugated web girders at the same magnitude of initial imperfection.

## REFERENCES

- [1] M. Elgaaly, A. Seshadri, and R. W. Hamilton, "Bending strength of steel beams with corrugated webs," *J. Struct. Eng.*, vol. 123, no. 6, pp. 772–782, 1997.
- [2] F. Hu, G. Shi, and Y. Shi, "Experimental study on seismic behavior of high strength steel frames: Global response," *Eng. Struct.*, vol. 131, pp. 163–179, 2017.
- [3] J. Wang, S. Afshan, M. Gkantou, M. Theofanous, C. Baniotopoulos, and L. Gardner, "Flexural behaviour of hot-finished high strength steel square and rectangular hollow sections," *J. Constr. Steel Res.*, vol. 121, pp. 97–109, 2016.

- 
- [4] Y. S. Choi, D. Kim, and S. C. Lee, "Ultimate shear behavior of web panels of HSB800 plate girders," *Constr. Build. Mater.*, vol. 101, pp. 828–837, 2015.
- [5] "[http://www.hera.org.nz/Story?Action=View&Story\\_id=1295;](http://www.hera.org.nz/Story?Action=View&Story_id=1295;)," 2013. .
- [6] A. F. Fraser, "Experimental investigation of the strength of multiweb beams with corrugated webs," *Tech. note 3801*, vol. 53, no. 9, pp. 1689–1699, 2013.
- [7] B. Kövesdi, B. Jáger, and L. Dunai, "Bending and shear interaction behavior of girders with trapezoidally corrugated webs," *J. Constr. Steel Res.*, vol. 121, pp. 383–397, 2016.
- [8] B. Jáger, L. Dunai, and B. Kövesdi, "Experimental investigation of the M-V-F interaction behavior of girders with trapezoidally corrugated web," *Eng. Struct.*, vol. 133, pp. 49–58, 2017.
- [9] B. Jáger, L. Dunai, and B. Kövesdi, "Girders with trapezoidally corrugated webs subjected by combination of bending, shear and path loading," *Thin-Walled Struct.*, vol. 96, pp. 227–239, 2015.
- [10] J. Lindner, "Zur Bemessung von Trapezstegträgern," *Der Stahlbau*, vol. 61, pp. 311–318, 1992.
- [11] DASt-Richtlinie 015, "Träger mit schlanken Stegen," *Stahlbau-Verlagsgesellschaft*, 1990.
- [12] R. P. Johnson and J. Cafolla, "Local flange buckling in plate girders with corrugated webs," *Proc. ICE - Struct. Build.*, pp. 148–156, 1997.
- [13] M. Dabon and A. S. Elamary, "Flange compactness effects on the behavior of steel beams with corrugated webs," *J. Eng. Sci.*, vol. 34, no. 5, pp. 1507–1523, 2006.
- [14] E. Y. Sayed-ahmed, "Design aspects of steel I-girders with corrugated steel webs," *Electron. J. Struct. Eng.*, vol. 7, pp. 27–40, 2007.
- [15] S. H. Lho, C. H. Lee, J. T. Oh, Y. K. Ju, and S. D. Kim, "Flexural capacity of plate girders with very slender corrugated webs," *Int. J. Steel Struct.*, vol. 14, no. 4, pp. 731–744, 2014.
- [16] G. Q. Li, J. Jiang, and Q. Zhu, "Local buckling of compression flanges of H-beams with corrugated webs," *J. Constr. Steel Res.*, vol. 112, pp. 69–79, 2015.
- [17] B. Jáger, L. Dunai, and B. Kövesdi, "Flange buckling behavior of girders with corrugated web Part I: Experimental study," *Thin-Walled Struct.*, vol. 118, no. April, pp. 181–195, 2017.
- [18] B. Jáger, L. Dunai, and B. Kövesdi, "Flange buckling behavior of girders with corrugated web Part II: Numerical study and design method development," *Thin-Walled Struct.*, vol. 118, no. April, pp. 238–252, 2017.
- [19] Dassault Systèmes Simulia, *Abaqus CAE User's Manual (6.12)*. 2012.
- [20] M. F. Hassanein and O. F. Kharoob, "Behavior of bridge girders with corrugated webs: (I) Real boundary condition at the juncture of the web and flanges," *Eng. Struct.*, vol. 57, pp. 554–564, 2013.
- [21] European Committee for Standardization, *EN 1993-1-5: Eurocode 3: Design of Steel Structures. Part 1-5: Plated Structural Elements*, vol. 3. 2007.
- [22] A. A. Elkawas, M. F. Hassanein, and M. H. El-Boghdadi, "Numerical investigation on the nonlinear shear behaviour of high-strength steel tapered corrugated web bridge girders," *Eng. Struct.*, vol. 134, pp. 358–375, 2017.

[23] R. G. Driver, H. H. Abbas, and R. Sause, "Shear Behavior of Corrugated Web Bridge Girders," *J. Struct. Eng.*, vol. 132, no. 2, pp. 195–203, 2006.

## دراسة عددية لسلوك انبعاج الشفة في الكمرات ذات الاعصاب المموجة ذات القطاع (I) المصنوعة من صلب عالي المقاومة

### الملخص العربي:

تم استخدام الكمرات اللوحية الفولاذية ذات العصب المموج ذو الشكل شبه المنحرف (TCWPGs) على مدار السنوات الماضية في العديد من الجسور الفولاذية للطرق والسكك الحديدية في جميع أنحاء العالم نظراً لأنها تتمتع بالعديد من المزايا الهامة إذا ما قورنت بالكمرات اللوحية ذات العصب المستوي. يعتمد التصميم المناسب للكمرات اللوحية ذات العصب المموج بشكل أساسي على مقاومة الانحناء والقص لهذه الكمرات. ومع ذلك، فإن مقاومة الانحناء تعد الأكثر أهمية. أيضاً لم يدرس العديد من الباحثين مقاومة الانحناء لمثل هذه الكمرات خاصةً عند انهيارها بواسطة إنبعاج الشفة المحلي (FLB) في هذه الكمرات ذات العصب المموج. في هذا البحث، تم فحص سلوك الإنبعاج المحلي للكمرات اللوحية الفولاذية ذات العصب المموج ذو الشكل شبه المنحرف المصنوعة من ألواح فولاذية عالية المقاومة (HSS) للحصول على مزايا كل من ألواح العصب المموج (CWPs) والفولاذ عالي المقاومة (HSSs) سوياً. تم إجراء دراسة بارامترية رقمية جديدة على أربعة متغيرات مهمة لتفسير والتحقيق في سلوك الإنبعاج المحلي لشفة الكمرات اللوحية المموجة الفولاذية عالية المقاومة، مع الأخذ في الاعتبار بشكل أساسي تأثيرات كل من نسبة سمك الشفة إلى سمك العصب وطول شفة الضغط وزاوية التمدد ومقدار التشوه الابتدائي لشفة الضغط على سلوك الكمرات ذات الأعصاب المموجة المصنوعة من صلب عالي المقاومة. باستخدام برنامج العناصر متناهية الصغر الشائع الاستخدام ABAQUS، تم الحصول على نتائج نماذج العناصر المتناهية الصغر لتحليلها ومناقشتها. أخيراً، تم تقديم بعض النصائح المهمة لمساعدة المهندسين الإنشائيين على تصميم مثل هذه الكمرات تحت أحمال الإنحناء بطريقة اقتصادية.